J. Mod. Transport. (2014) 22(1):1–11
DOI 10.1007/s40534-013-0025-8

www.springer.com/40534

Study on calculation of rock pressure for ultra-shallow tunnel in poor surrounding rock and its tunneling procedure

Xiaojun Zhou · Jinghe Wang · Bentao Lin

Received: 27 June 2013 / Revised: 3 November 2013 / Accepted: 5 November 2013 / Published online: 30 November 2013

Abstract A computational method of rock pressure applied to an ultra-shallow tunnel is presented by key block theory, and its mathematical formula is proposed according to a mechanical tunnel model with super-shallow depth. Theoretical analysis shows that the tunnel is subject to asymmetric rock pressure due to oblique topography. The rock pressure applied to the tunnel crown and sidewall is closely related to the surrounding rock bulk density, tunnel size, depth and angle of oblique ground slope. The rock pressure applied to the tunnel crown is much greater than that to the sidewalls, and the load applied to the left sidewall is also greater than that to the right sidewall. Meanwhile, the safety of the lining for an ultra-shallow tunnel in strata with inclined surface is affected by rock pressure and tunnel support parameters. Steel pipe grouting from ground surface is used to consolidate the unfavorable surrounding rock before tunnel excavation, and the reinforcing scope is proposed according to the analysis of the asymmetric load induced by tunnel excavation in weak rock with inclined ground surface. The tunneling procedure of bench cut method with pipe roof protection is still discussed and carried out in this paper according to the special geological condition. The method and tunneling procedure have been successfully utilized to design and drive a real expressway tunnel. The practice in building the super-shallow tunnel has proved the feasibility of the calculation method and tunneling procedure presented in this paper.

Keywords Ultra-shallow tunnel · Asymmetric rock pressure · Surrounding rock · Rock treatment · Tunneling method

X. Zhou (✉) · J. Wang
Key Laboratory of Transportation Tunnel Engineering of Ministry of Education, School of Civil Engineering, Southwest Jiaotong University, Chengdu 610031, China
e-mail: Zhouxjyu69@163.com; Zhouxjyu69@sina.com

B. Lin
The 2nd Institute of Civil and Architecture Engineering, China Railway Eryuan Engineering Corporation Ltd., Chengdu 610031, China

1 Introduction

The fast development of economy requires much more rapid and convenient transportation systems. Therefore, expressways and high speed railways have been built in China. Since the most land of western and northern China belongs to mountainous area, it is extremely difficult to build railways and expressways in these regions. If a transportation line such as highway or railway will be built in mountainous areas, tunnels are frequently adopted to overcome height barriers in the line. When the conditions of the area where transportation lines pass through is complicated in geology and topography, special geological problems might be encountered during the design and construction of transportation tunnels. If the ground has inclined topography, namely the ground surface appears in oblique form, then tunnel is easily subject to asymmetric rock pressure and its support structure must be excogitated according to asymmetric rock pressure.

In order to realize rational design and safe construction of mountainous tunnels, many studies and experiments have been carried out by scholars across the world. Goodman et al. [1] investigated the modeling techniques of tunnels in jointed rock, and presented an experimental and a numerical method to analyze the tunnel excavation in jointed rockmass. Shen and Barton [2] analyzed the disturbed zone around tunnels in jointed rock mass; they

classified the disturbed zone into failure, open, and shear ones around a tunnel in jointed rock mass. Zhou et al. [3] made an insight into the rock pressure on tunnel with shallow depth in geologically inclined bedding strata, and set up formulas to calculate the asymmetric rock pressure applied to a tunnel with shallow depth in stratified rock. Later, Zhou and Yang [4] discussed the asymmetric rock pressure applied to the shallow tunnel in strata with inclined ground surface, and proposed a method to calculate the asymmetric rock pressure applied to the tunnel in strata with inclined ground surface by key block theory. Yang et al. [5] analyzed the calculation of rock pressure applied to three tunnels with large transection and small neighborhood in shallow surrounding rock; they suggested that the conventional method to calculate the rock pressure applied to shallow tunnel with small neighborhood should be improved. He et al. [6] studied the asymmetrical load effect on tunnels in geologically inclined bedding strata. They found that the rock pressure at the left wall of a tunnel is greater than that at the right wall. As the dip angle of bedding strata increases, the asymmetrical load gradually tends to be symmetric. In Zhou's [7] recent research, he studied the method to calculate the rock pressure for shallow asymmetric tunnel, and presented a method to determine a proper depth for shallow asymmetric tunnel in strata with inclined ground surface.

Most of studies available focused on the stability and deformation of tunnels and surrounding rock in jointed rockmass. Only a few concerned the calculation method of rock pressure applied to shallow tunnel [8, 9]. When designing tunnel structures, the rock pressure applied to tunnel lining is often obtained by numerical simulation or field monitoring. However, this is often hard for designers to use. To date, the calculation method of asymmetric rock pressure applied to super-shallow tunnel in strata with inclined ground surface has not been addressed [10]. As we know, the most difficult problem during design and construction of a tunnel in strata with inclined topography is to deal with the extremely thin overburden depth. This means that an ultra-shallow-tunnel will be excogitated and built in strata with inclined geomorphology; consequently, the influence of rock excavation will extend to ground surface and possibly cause casualties during tunneling [11, 12].

This paper aims to find out a simple way to calculate the asymmetric rock pressure for design of tunnel lining in super-shallow surrounding rock. The driving procedure for the bored tunnel is determined, taking into account the poor geological condition. Finally, a typical ultra-shallow tunnel for an expressway in Sichuan, China was taken as an example to make its structural design and safe construction procedure, which verifies the effectiveness of the proposed method.

2 Analysis of asymmetric rock pressure applied to super-shallow tunnel

In order to analyze the asymmetric load on the tunnel support with an ultra-shallow depth in strata with inclined ground surface, a mechanical model is set up according to the geological and topographical condition of a vehicular tunnel named Zagunao with two lanes in an expressway in Sichuan, the southwest province of China, as shown in Fig. 1.

According to the normal structural design of expressway tunnel with two lanes, the upper part of its reinforced

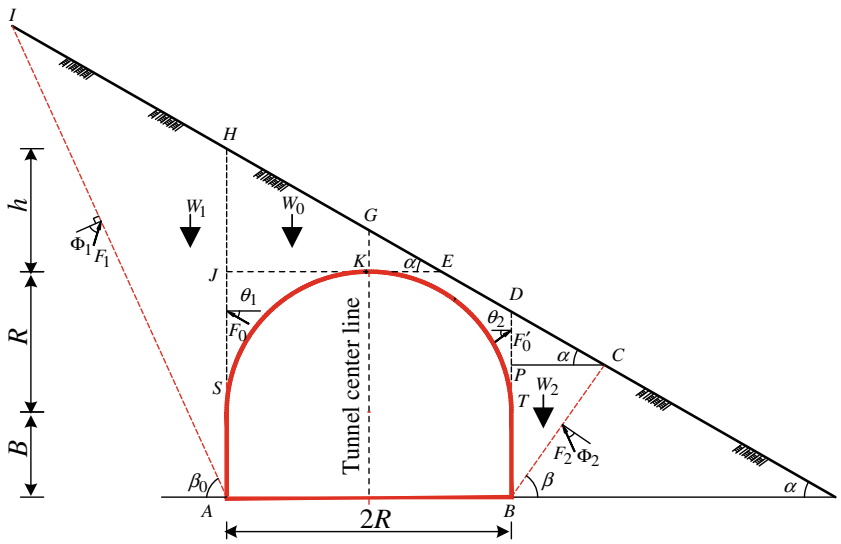

Fig. 1 Mechanical model of ultra-shallow tunnel

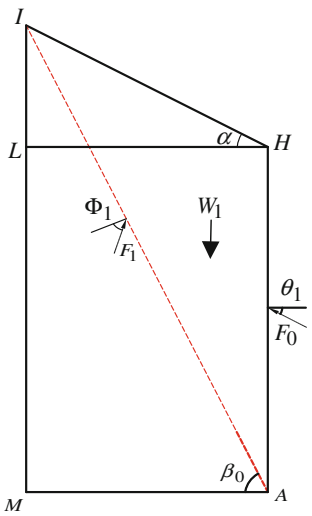

Fig. 2 Geometric relation of angle α and β_0

concrete lining from its spring line appears in semi-circular arch with a radius of R and a width of $2R$. Since the tunnel has an ultra-shallow overburden depth, excavation of surrounding rock must cause ground subsidence and its influence will extend to the surface. If it is supposed that there exist two breaking planes in the surrounding rock on each side of the tunnel, namely plane BC and plane AI, then the surrounding rock in ΔBCD and ΔAHI may tend to descend downward due to its rock gravity; synchronously, the surrounding rock above the tunnel crown namely in ΔJEH may also be caused to descend along breaking planes BD and AH by gravity as the tunnel will be driven. However, friction resistances must exist on each fracture plane; frictions will impede the slide of the surrounding rock in each triangular block. Let the surrounding rock in blocks exist in a critical equilibrium state; then their mechanical relations can be derived from Fig. 1.

In ΔAHI, the gravity W_1 of the surrounding rock circumscribed by block AHI is derived from the geometric relation as shown in Fig. 2, i.e.,

$$W_1 = \frac{1}{2}\gamma_1(h + R + B)^2, \tag{1}$$

where α denotes the slope angle and β_0 the breaking angle between planes AI and MA, in degrees; γ_1 stands for the bulk density of the surrounding rock in block AHI, in kN/m^3; and other symbols are delineated in Figs. 1 and 2.

In addition, three forces F_1, W_1, and F_0 constitute a vector triangle as shown in Fig. 3, where F_1 denotes the friction resistance applied to plane AI, F_0 the friction resistance to plane AH, and W_1 the gravity of the surrounding rock enclosed by block AHI. We can deduce from Fig. 3 by sine theorem that

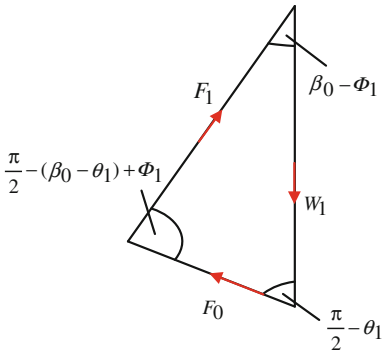

Fig. 3 Vector triangle of forces F_1, W_1, and F_0

$$\frac{F_0}{\sin(\beta_0 - \phi_1)} = \frac{W_1}{\sin\left[\frac{\pi}{2} - (\beta_0 - \theta_1) + \phi_1\right]}. \tag{2}$$

Substituting Eq. (1) into Eq. (2), we obtain

$$F_0 = \frac{\gamma_1(h + R + B)^2}{2\cos\theta_1} \cdot \frac{1}{\tan\beta_0 - \tan\alpha} \times \frac{\tan\beta_0 - \tan\phi_1}{1 + \tan\beta_0\tan\phi_1 + \tan\theta_1(\tan\beta_0 - \tan\phi_1)}. \tag{3}$$

Equation (3) shows that the friction resistance applied to breaking plane AH varies with the breaking angle β_0, so F_0 may get its maximum or minimum value as β_0 varies within 90°. Thus, if let

$$\lambda = \frac{1}{\tan\beta_0 - \tan\alpha} \times \frac{\tan\beta_0 - \tan\phi_1}{1 + \tan\beta_0\tan\phi_1 + \tan\theta_1(\tan\beta_0 - \tan\phi_1)}, \tag{4}$$

then Eq. (3) is converted into

$$F_0 = \frac{\gamma_1(h + R + B)^2}{2} \cdot \frac{\lambda}{\cos\theta_1}. \tag{5}$$

In order to get the extreme value of F_0, let

$$\frac{\partial F_0}{\partial \beta_0} = 0. \tag{6}$$

Then the following expression is derived:

$$\tan^2\beta_0 - 2\tan\phi_1\tan\beta_0 - \frac{\tan\phi_1 - \tan\alpha - (\tan\theta_1 + \tan\alpha)\tan^2\phi_1}{\tan\phi_1 + \tan\theta_1} = 0. \tag{7}$$

Equation (7) represents a quadratic equation with one variable β_0, and its maximum root is derived as follows:

$$\tan\beta_0 = \tan\phi_1 + \sqrt{\frac{(\tan\phi_1 - \tan\alpha)(1 + \tan^2\phi_1)}{\tan\phi_1 + \tan\theta_1}}. \tag{8}$$

It is known from Eq. (8) that the maximum β_0 for breaking plane AI is controlled by angle ϕ_1, α, and θ_1.

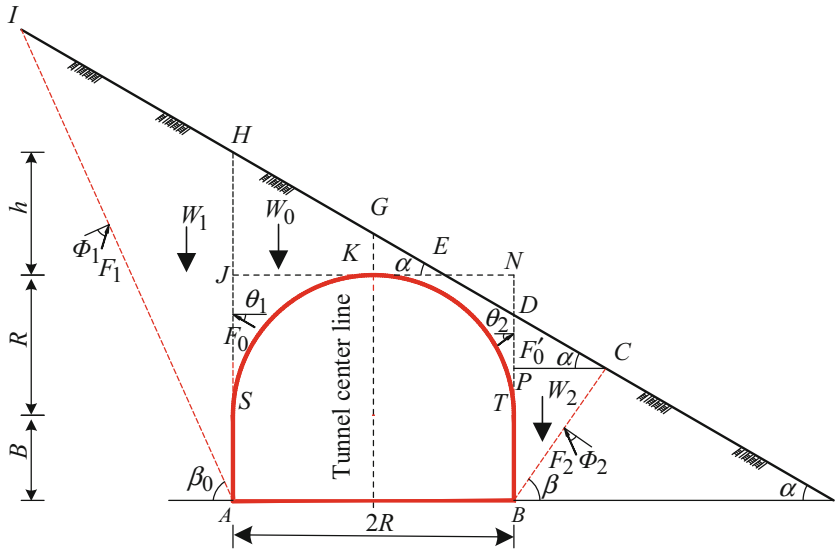

Fig. 4 Geometric relation of ΔBDC and ΔDPC

As for the triangular block BCD shown in Fig. 1, the surrounding rock may also slide along the fracture planes BC and BD due to its gravity W_2. In order to anatomize the friction resistance applied to breaking plane BD, the gravity W_2 must be obtained. Therefore, if extend straight line KE to point N, and line TD to N, then point N is the intersection between line EN and DN, as shown in Fig. 4.

In ΔHJE, since $HJ = h$ and $JE = h{\cdot}\mathrm{c}\tan\alpha$, we have

$$EN = 2R - h \cdot \mathrm{c}\tan\alpha. \tag{9}$$

Furthermore, in ΔEDN, we have $ND = 2R\tan\alpha - h$, and $BD = B{+}R - (2R\tan\alpha - h)$. Thus, there is

$$BD = B + h + R(1 - 2\tan\alpha). \tag{10}$$

In addition, both ΔDPC and ΔBCP are in right triangles; therefore, following relations may exist, i.e.,

$$\tan\alpha = \frac{DP}{PC}, \tag{11}$$

$$\tan\beta = \frac{PB}{PC}, \tag{12}$$

$$PB = BD - DP. \tag{13}$$

Substituting Eqs. (11) and (12) into Eq. (13), we get

$$PC = \frac{B + h + R(1 - 2\tan\alpha)}{\tan\alpha + \tan\beta}. \tag{14}$$

Therefore, the gravity W_2 of the triangular block BCD is derived as

$$W_2 = \frac{\gamma_2}{2}\frac{[B + h + R(1 - 2\tan\alpha)]^2}{\tan\alpha + \tan\beta}, \tag{15}$$

where γ_2 denotes the bulk density of the surrounding rock within the block BCD.

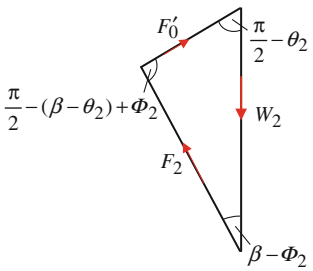

Fig. 5 Vector triangle of forces F_2, W_2, and F_0'

Similarly, the three forces F_2, W_2, and $F_0^{'}$ also constitute a vector triangle as shown in Fig. 5 and their relation is as follows:

$$\frac{F_0^{'}}{\sin(\beta - \phi_2)} = \frac{W_2}{\sin\left[\frac{\pi}{2} - (\beta - \theta_2) + \phi_2\right]}. \tag{16}$$

Substituting Eq. (15) into Eq. (16), we get

$$F_0^{'} = \frac{\gamma_2[B + h + R(1 - 2\tan\alpha)]^2}{2\cos\theta_2} \cdot \frac{1}{\tan\beta + \tan\alpha} \times \frac{\tan\beta - \tan\phi_2}{1 + \tan\beta\tan\phi_2 + \tan\theta_2(\tan\beta - \tan\phi_2)}. \tag{17}$$

It is known from Eq. (17) that the friction resistance $F_0^{'}$ applied to the breaking plane BD varies with the breaking angle β, so it may get an extreme value as β varies within 90°. Let

$$\lambda^{'} = \frac{1}{\tan\beta + \tan\alpha} \times \frac{\tan\beta - \tan\phi_2}{1 + \tan\beta\tan\phi_2 + \tan\theta_2(\tan\beta - \tan\phi_2)}. \tag{18}$$

Then Eq. (17) is converted into

$$F_0' = \frac{\gamma_2[B + h + R(1 - 2\tan\alpha)]^2}{2} \cdot \frac{\lambda'}{\cos\theta_2}. \tag{19}$$

To derive the extreme value of F_0', let

$$\frac{\partial F_0'}{\partial \beta_0} = 0. \tag{20}$$

Then we obtain

$$\tan^2\beta - 2\tan\phi_2\tan\beta - \frac{\tan\phi_2 + \tan\alpha - (\tan\theta_2 + \tan\alpha)\tan^2\phi_2}{\tan\phi_2 + \tan\theta_2} = 0. \tag{21}$$

Equation (21) is also a quadratic equation with one variable β, so its maximum root is derived as follows:

$$\tan\beta = \tan\phi_2 + \sqrt{\frac{(\tan\alpha + \tan\phi_2)(1 + \tan^2\phi_2)}{\tan\phi_2 + \tan\theta_2}}. \tag{22}$$

Equation (22) shows that the failure angle β is closely related to angles ϕ_2, θ_2, and α. As for the vertical load applied on the crown of the tunnel, W_0 contributes the great proportion. If the surrounding rock above its crown tends to slide along the assumed planes AH and BD, it will be resisted by the vertical components of friction resistance F_0 and F_0'. Their vertical components are derived as follows:

$$F_{0v} = \frac{\gamma_1}{2}(B + h + R)^2\lambda\tan\theta_1, \tag{23}$$

$$F_{0v}' = \frac{\gamma_2}{2}[B + h + R(1 - 2\tan\alpha)]^2\lambda'\tan\theta_2. \tag{24}$$

Then the downward load applied to the crown of the tunnel is

$$Q = W_0 - (F_{0v} + F_{0v}'), \tag{25}$$

where W_0 stands for the gravity of the surrounding rock above the tunnel crown, in kN; its mathematical expression can be derived from the geometrical relation as shown in Fig. 1. The gravity of the surrounding rock above the tunnel crown is obtained by deducting the area of tunnel transection from the area of trapezoid $ABDH$, namely the area above the tunnel crown is as follows

$$A = \frac{(AH + BD)}{2} \cdot AB - AB \cdot AS - \frac{\pi R^2}{2}. \tag{26}$$

Then gravity W_0 is obtained as follows:

$$W_0 = 2\gamma_0 Rh + 2\gamma_0 R^2(1 - \tan\alpha) - \frac{\gamma_0}{2} \cdot \pi R^2, \tag{27}$$

where γ_0 stands for the bulk density of the surrounding rock above the tunnel crown, in kN/m^3.

Substitution of Eqs. (23), (24), and (27) into (25) yields

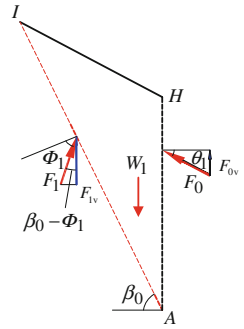

Fig. 6 Vertical components of F_1 and F_0

$$Q = 2\gamma_0 Rh + 2\gamma_0 R^2(1 - \tan\alpha) - \frac{\gamma_0}{2} \cdot \pi R^2 - \frac{\gamma_1}{2}(B + h + R)^2\lambda\tan\theta_1 - \frac{\gamma_2}{2}[B + h + R(1 - 2\tan\alpha)]^2\lambda'\tan\theta_2. \tag{28}$$

Then the vertical downward pressure applied to the crown is

$$q = \frac{Q}{2R}. \tag{29}$$

Substituting Eq. (28) into Eq. (29), we obtain the rock pressure applied on the tunnel crown as follows:

$$q = \gamma_0 h + \gamma_0 R(1 - \tan\alpha) - \frac{\gamma_0}{4}\pi R - \frac{\gamma_1}{4R}(B + h + R)^2\lambda\tan\theta_1 - \frac{\gamma_2}{4R}[B + h + R(1 - 2\tan\alpha)]^2\lambda'\tan\theta_2. \tag{30}$$

Equation (30) shows that the vertical pressure applied to the tunnel crown caused by gravity W_0 is related to parameters such as γ_0, h, α, β, R, θ_1, and θ_2; and its direction is always downward.

According to Fig. 1, the surrounding rock enclosed by ΔAHI and ΔBCD exert a lateral rock thrust on two side walls of the tunnel. As for ΔAHI, the lateral load applied to the side wall is derived as follows.

In ΔAHI as shown in Fig. 6, according to the division of forces, the vertical component of friction resistance can be obtained. According to Fig. 3, there exists sine theorem, namely

$$\frac{F_1}{\sin\left(\frac{\pi}{2} - \theta_1\right)} = \frac{F_0}{\sin(\beta_0 - \phi_1)}. \tag{31}$$

Then friction resistance F_1 is

$$F_1 = \frac{\gamma_1}{2}(B + h + R)^2\frac{\lambda}{\sin(\beta_0 - \phi_1)}. \tag{32}$$

In addition, the sine theorem also holds in Fig. 5, and there is a relation as follows:

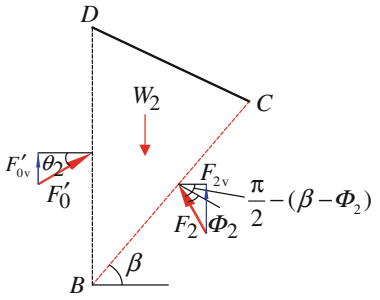

Fig. 7 Vertical components of $F_0^{'}$ and F_2

$$\frac{F_2}{\sin\left(\frac{\pi}{2}-\theta_2\right)}=\frac{F_0^{'}}{\sin(\beta-\phi_2)}. \tag{33}$$

And the friction resistance F_2 is

$$F_2=\frac{\gamma_2}{2}[B+h+R(1-2\tan\alpha)]^2\frac{\lambda^{'}}{\sin(\beta-\phi_2)}. \tag{34}$$

The vertical components of friction resistance F_1 and F_2 tends to prevent the surrounding rock both in block *AHI* and *BCD* from sliding along the assumed fracture plane. The vertical components of F_1 and F_2 are as follows:

$$F_1\mathrm{v}=F_1\cos(\beta_0-\phi_1), \tag{35}$$

$$F_2\mathrm{v}=F_2\sin\left[\frac{\pi}{2}-(\beta-\phi_2)\right]. \tag{36}$$

Substitution of Eqs. (32) and (34) into Eqs. (35) and (36) yields the following expressions:

$$F_{1\mathrm{v}}=\frac{\gamma_1}{2}(B+h+R)^2\frac{\lambda}{\tan(\beta_0-\phi_1)}, \tag{37}$$

$$F_{2\mathrm{v}}=\frac{\gamma_2}{2}[B+h+R(1-2\tan\alpha)]^2\frac{\lambda^{'}}{\tan(\beta-\phi_2)}. \tag{38}$$

As for block *AHI*, the downward load Q_1 is derived as

$$Q_1=W_1-(F_{1\mathrm{v}}+F_{0\mathrm{v}}). \tag{39}$$

Thus, the downward load Q_1 caused by gravity W_1 is derived as

$$Q_1=\frac{\gamma_1}{2}(B+h+R)^2\times\left[\frac{1}{\tan\beta_0-\tan\alpha}-\frac{\lambda}{\tan(\beta_0-\phi_1)}-\lambda\tan\theta_1\right]. \tag{40}$$

If Q_1 is totally applied to the left side wall, then the lateral pressure (e_1) applied to the left side wall *AS* is derived as

$$e_1=\frac{\gamma_1}{2B}(B+h+R)^2\eta, \tag{41}$$

where η is the lateral pressure coefficient, and its specific expression is as follows:

$$\eta=\frac{1}{\tan\beta_0-\tan\alpha}-\frac{\lambda}{\tan(\beta_0-\phi_1)}-\lambda\tan\theta_1. \tag{42}$$

For the lateral load applied to the right side wall of the tunnel, the forces and their relation are shown in Fig. 7.

According to the relation between gravity and friction resistances in Fig. 7, the downward load Q_2 is derived as

$$Q_2=W_2-(F_{2\mathrm{v}}+F_{0\mathrm{v}}^{'}). \tag{43}$$

If Eqs. (24) and (36) are substituted into Eq. (43), then the downward load Q_2 caused by gravity W_2 is also obtained as

$$Q_2=\frac{\gamma_2}{2}[B+h+R(1-2\tan\alpha)]^2\times\left[\frac{1}{\tan\beta+\tan\alpha}-\frac{\lambda^{'}}{\tan(\beta-\phi_2)}-\lambda^{'}\tan\theta_2\right]. \tag{44}$$

Then, the lateral pressure (e_r) applied to the right side wall *BD* is

$$e_r=\frac{\gamma_2}{2B}[B+h+R(1-2\tan\alpha)]^2\eta^{'}, \tag{45}$$

where $\eta^{'}$ denotes lateral pressure coefficient, and its mathematical expression is as follows:

$$\eta^{'}=\frac{1}{\tan\beta+\tan\alpha}-\frac{\lambda^{'}}{\tan(\beta-\phi_2)}-\lambda^{'}\tan\theta_2. \tag{46}$$

To sum up, the method to calculate the rock pressure applied to an ultra-shallow tunnel in strata with inclined ground has been derived from above analysis. It is apparent that the lateral pressure applied to two side walls of the tunnel is not identical. Therefore, a tunnel with ultra-shallow depth undergoes asymmetric rock pressure.

3 Calculation of asymmetric rock pressure for an expressway tunnel

In order to analyze the rock pressure applied to an typical ultra-shallow tunnel, Zagunao tunnel in an expressway of Sichuan province in China is analyzed; its typical geological transection is shown in Fig. 8. There are two tunnels in the expressway; both are separated from each other. The net distance from outside wall of the left tunnel to that of the right tunnel is only 20 m. The main feature of this expressway tunnel is that its entry portal section lies in strata with a shallow and ultra-shallow overburden due to the requirement of line development.

Each tunnel has two vehicular lanes. The total length of the entry portal section with shallow depth is 25 m long in its longitudinal direction. In this shallow section, the left belongs to deep tunnel with an overburden from 13 to 36 m, but the right one has a very thin overburden that

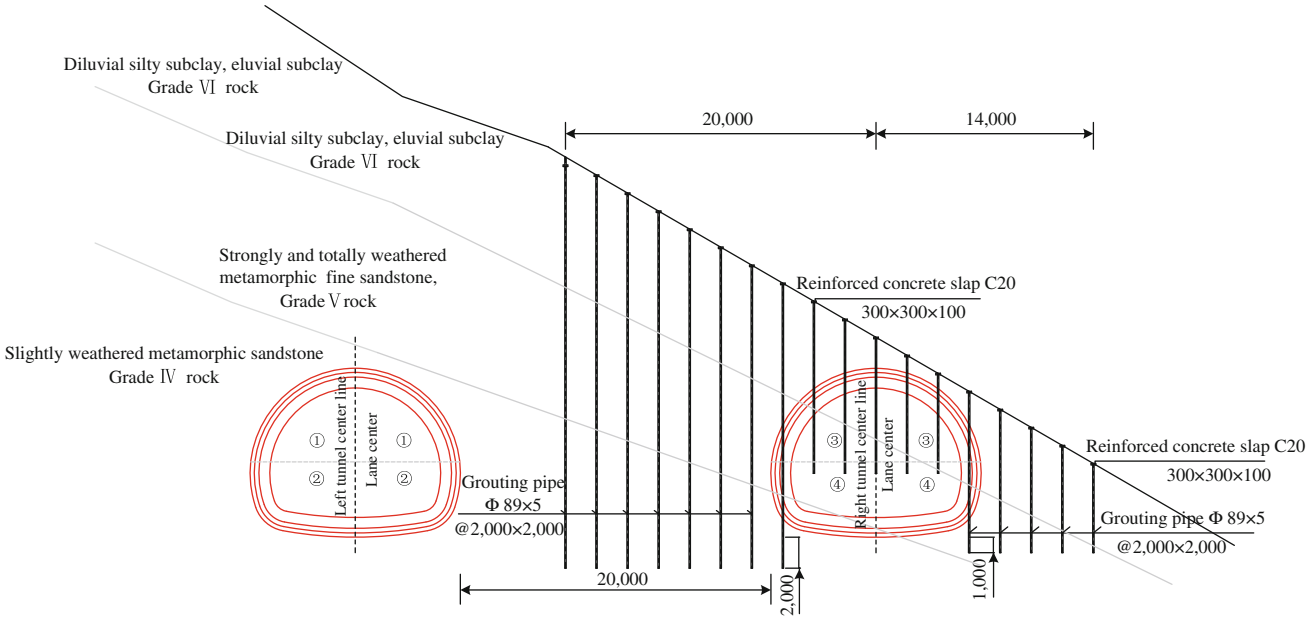

Fig. 8 Geological transection of an ultra-shallow tunnel in entry portal section (unit: mm)

Table 1 Basic parameters of the surrounding rock and tunnel

γ_0 (kN/m^3)	γ_1 (kN/m^3)	γ_2 (kN/m^3)	θ_1 (°)	θ_2 (°)	ϕ_1(°)	ϕ_1(°)	α(°)	B (m)	R (m)	h (m)
15	16	14	20	18	40	35	28	4.11	6.77	6.0

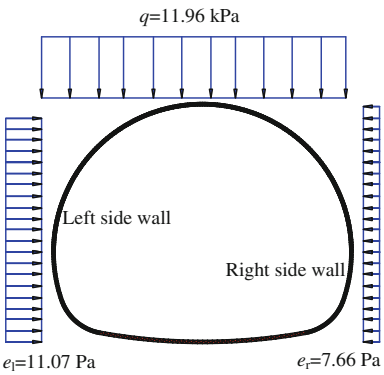

Fig. 9 Rock pressure applied to tunnel support

varies from 2 to 18 m. The surrounding rock mainly falls into diluvial silty subclay, eluvial subclay, and strongly weathered metamorphic fine sandstone. According to the Rock Quality Designation (RQD) and Basic Quality (BQ) system for rock mass classification [13, 14], and the *Code for Design of Highway Tunnel*, the surrounding rock belongs to grades IV, V, and VI [15, 16].

In order to make a concise analysis and simplify the computation process of the surrounding rock pressure, let all surrounding rock belong to grade VI. The physical and mechanical parameters of the surrounding rock and the basic size of the tunnel are shown in Table 1. Although this hypothesis seems to be simple, the result is still representative.

Substituting all the parameters in Table 1 into the above-stated equations, we derived the rock pressure applied to the ultra-shallow tunnel, as shown in Fig. 9.

It is clear from Fig. 9 that the right tunnel is subject to asymmetric pressure; and its crown is subject to the maximum vertical pressure with downward direction. The rock pressure applied to its left sidewall is greater than that to the right one in magnitude, but smaller than that on its crown. In addition, if these parameters are substituted into Eqs. (8) and (22), then the breaking plane angle are obtained as $\beta_0 = 56.28°$ and $\beta = 63.86°$. This indicates that excavation of the surrounding rock inside the tunnel contour may possibly cause overburden rock to slide or subside along the assumed breaking plane as shown in Fig. 10.

In order to illustrate the assumed plane of the surrounding rock, the arc invert of the tunnel is simplified to a straight floor but this does not affect the analysis of rock pressure.

According to the calculated results of the rock pressure applied to tunnel and the assumed fracture plane, the structural design of the ultra-shallow tunnel and its ground

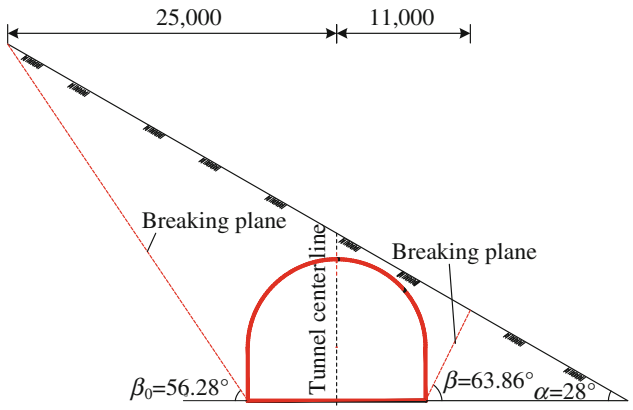

Fig. 10 Slide plane of the surrounding rock (unit: mm)

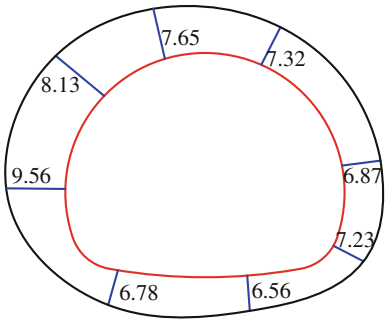

Fig. 12 Safety factor of primary support

treatment for the right tunnel have been carried out. The tunnel support and its designed parameters are shown in Fig. 11 in detail.

The tunnel is supported with composite lining which consists of primary support and inner lining. According to the load and structure model in structure mechanics [15, 16], the internal forces in the primary and secondary support are calculated. By assuming the rock pressure calculated by the method presented in this paper is totally applied to the primary support, the safety factors in the typical cross section of the primary support is obtained by allowable stress design and ultimate strength design method [15, 16]. The obtained results for primary support are shown in Fig. 12. Since the minimum safety factor reaches 6.56, the designed primary support is safe when it is subject to asymmetric rock pressure. In addition, if all the pressure is applied to the inner lining, then safety factors of the secondary lining are also calculated by using the same model as shown in Fig. 13. It is apparent that the secondary lining is also secure when it is subject to asymmetric rock pressure.

According to the rock pressure calculation of the ultra-shallow tunnel, the surrounding rock above the tunnel vault tends to slide along the two assumed fracture planes, and it will result in ground subsidence; therefore, ground treatment should be conducted in light of the above calculated

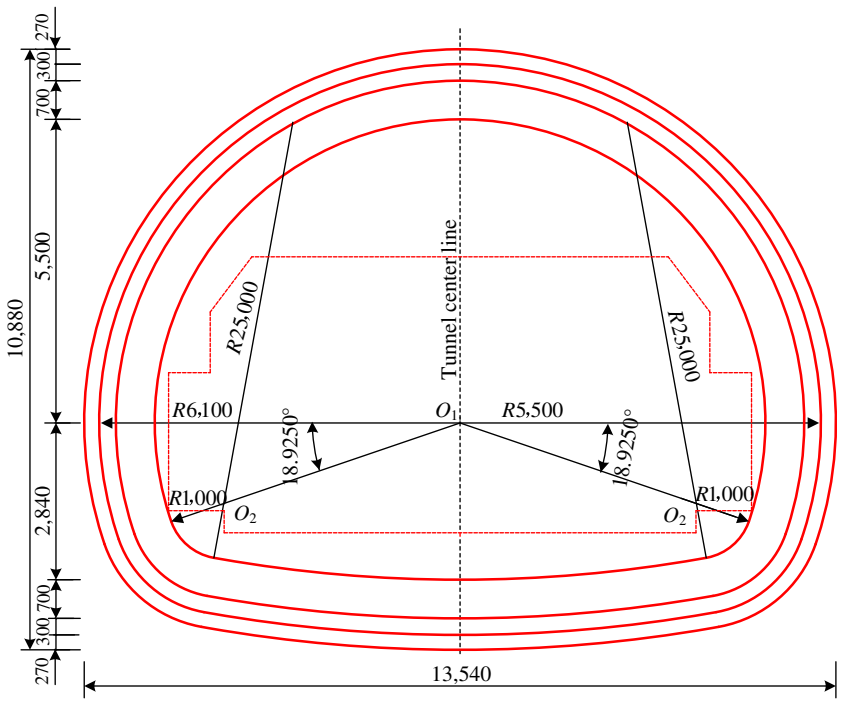

Fig. 11 Tunnel support and its transection (unit: mm). Grouting pipe ϕ42 mm × 5 mm, L = 4,500 mm @400 mm; Hollow grouting bolt ϕ25, L = 6,000 mm @300; I-shaped steel arch, I20, longitudinal @600 mm. Shotcrete, C25, δ = 270, ϕ8 steel mesh @150 × 150. Allowable camber 300 mm. Geotextile 350 g/m^2, δ = 1.2 mm PVC-P. Reinforced concrete, C25, δ = 700 mm

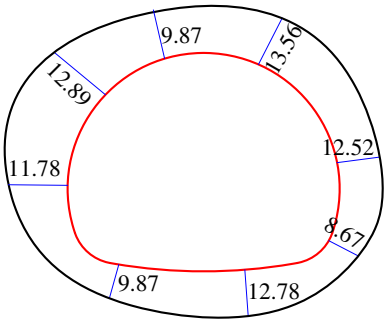

Fig. 13 Safety factors of inner lining

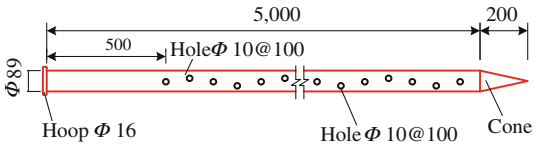

Fig. 14 Detail of grouting pipe (unit: mm)

results so as to lessen the rock settlement and construction risk during tunneling [17, 18]. According to the calculated maximum fracture angle of plane shown in Fig. 10, the ground treatment range must be greater than the subsidence scope; in addition, the supposed slide planes must also be consolidated. In consideration of the geology and geomorphology of the tunnel, cement grouting method is adopted to reinforce the surrounding rock with steel pipes from the ground surface. Since sandstone possesses large porosity, grouting can effectively enhance its shear strength; the detail of the grouting pipe is shown in Fig. 14. Since the portal section of the right tunnel is 25 m long in its longitudinal direction, cement grouting was carried out only in this section.

In order to analyze the effect of cement grouting in strata, the friction angle of the slide plane will be raised after cement grouting in the surrounding rock with steel pipes from ground surface. This means that their value will be enhanced. If the computational friction angle of the surrounding rock rises to $\phi_1 = 55^\circ$ and $\phi_2 = 50^\circ$, then $\theta_1 = 38.5^\circ$ and $\theta_2 = 35^\circ$. If these parameters are substituted into Eqs. (8) and (22), then the maximum fracture angles are obtained as $\beta_0{}' = 68.47^\circ$ and $\beta' = 69.51^\circ$. By comparing this result with the angle of slide plane before grouting, we obtain their relations as follows

$$\beta_0' = 1.22\beta_0, \tag{47}$$

$$\beta' = 1.09\beta. \tag{48}$$

This apparently shows that the shear strength of the surrounding rock gets enhanced after the ground has been reinforced with cement grouting. A comparison of ground treatment effect is shown in Fig. 15. From Fig. 15 we can infer that the vertical and lateral rock pressure applied to the tunnel support decrease largely as well after the surrounding rock is treated with steel pipe grouting from ground surface.

During the operation of in situ grouting, the grouting pressure must be kept within 1.0–1.5 MPa. In view of the in situ surface condition and ground geology at the tunnel site, the actual ground treatment and the details of designed parameters and grouting scope are shown in Fig. 8. Since the right tunnel more approaches to the ultra-shallow depth in the strata in comparison with the right one, ground

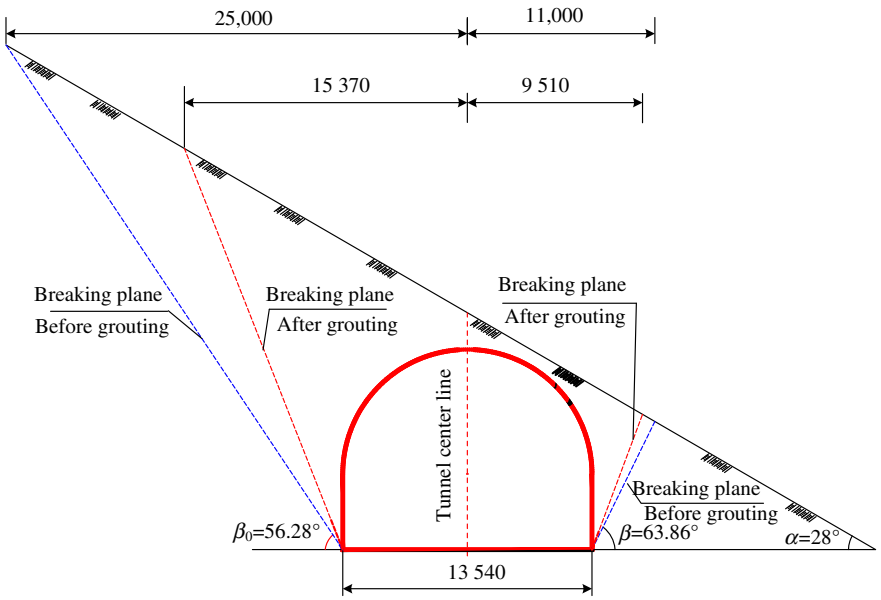

Fig. 15 Effect of ground treatment by cement grouting (unit: mm)

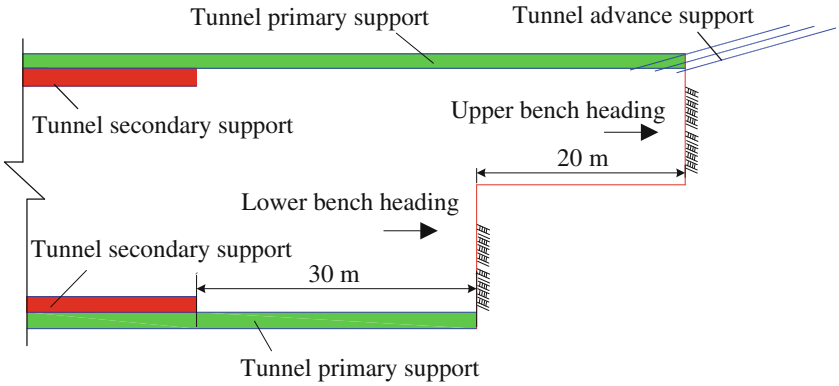

Fig. 16 Conventional tunneling process

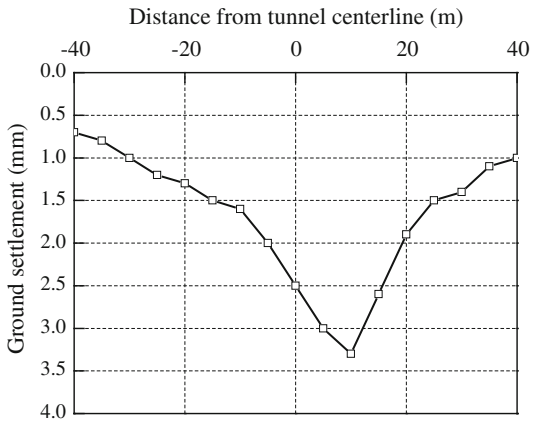

Fig. 17 Ground settlement due to tunnel excavation

treatment was only performed in its surrounding rock. As the left tunnel is deeply buried and the net distance between the two tunnels reaches 20 m, there is no need to treat the surrounding rock around the right tunnel.

4 Construction procedure of the ultra-shallow tunnel

The surrounding rock around the two expressway tunnels falls into three grades in terms of its uniaxial compressive strength and lithological integrity, namely, grades IV, V, and VI according to its RQD [12, 13]. The main lithology comprises sub-clay and metamorphic sandstone. The upper strata belongs to diluvial silty subclay and eluvial subclay, the middle strata belongs to totally and strongly weathered metamorphic fine sandstone, and the lower strata exists in slightly weathered metamorphic sandstone. Furthermore, the maximum area of tunnel transection amounts to 123 m^2, and the maximum tunnel span reaches 13.54 m. Since the left tunnel has higher overburden depth than the right one, in order to reduce tunneling risk such as rock collapse and cave-in, the two tunnels are driven with the conventional drill and blast method. The excavation sequence of the surrounding rock inside tunnel contour is divided into four main steps. First, the left tunnel is excavated, and then the right one. The detailed construction process and its support system are both shown in Fig. 8. The whole working face of each tunnel is divided into two parts, first the upper part is headed, and then the lower part: The circled digits in Fig. 8 represent the tunneling sequence of the surrounding rock within the tunnel contour by conventional tunneling method [18–20]. The longitudinal profile of the tunnel construction process is shown in Fig. 16.

During the construction period, in situ ground settlement was measured in order to analyze the ground subsidence. The monitored final settlement of ground is shown in Fig. 17.

It is known from Fig. 17 that the maximum value of ground settlement reaches 3.7 mm; it does not occur at the center point above the tunnel crown, and just takes place at the point 5 m away from centerline. This phenomenon is principally caused by uneven pressure in the surrounding rock. It must be mentioned that the ground settlement was measured after the ground treatment had been completed. The measurement reflects that performing ground treatment and tunnel primary support has achieved a desired effect. Therefore, the ground treatment, tunnel support, and tunneling procedure are practicable.

Through the above technical scenario, the construction of Zagunao tunnel, a typical ultra-shallow expressway tunnel in Sichuan Province, has been successfully completed. During its whole construction process, no disaster or safety accident occurred. This, in turn, verified that the design and construction program for the ultra-shallow expressway tunnel was feasible; furthermore, the goal of safe and economical construction for the ultra-shallow tunnel was fulfilled.

5 Conclusions

This paper mainly deals with the calculation of rock pressure for ultra-shallow tunnel and its ground treatment,

including its construction procedure. For this kind of tunnel, the rock pressure applied to the tunnel support is related to parameters such as ground slope angel α, rock fracture angle β, tunnel size B, R, H, and its depth h. After theoretical analysis on the calculation method of asymmetric rock pressure, the ground treatment of ultra-shallow tunnel and its tunneling procedure, some useful conclusions can be drawn as follows.

(1) The vertically downward load caused by gravity of the surrounding rock above the tunnel crown is much greater than the lateral load applied to tunnel side walls. When calculating the lateral pressure applied to super-shallow tunnel sidewalls, its value is mainly derived from the lateral surrounding rock, not from the surrounding rock above the tunnel crown. This is an innovative outcome in comparison with conventional methods.
(2) The rock pressure applied to the left sidewall is greater than that applied to the right one, and the lateral forces are not identical; therefore, the tunnel is subject to asymmetric pressure under ultra-shallow depth in topographically inclined strata.
(3) As for expressway tunnels, if there are two tunnels in a trunk line, and the external tunnel lies in an ultra-shallow condition, then its support should be designed according to the ultra-shallow condition, and the internal tunnel can be designed in terms of in situ geological condition. The construction method is determined in accordance with surrounding rock conditions. In order to control ground settlement, and keep safe tunneling, the priority of excavation should be given first to internal tunnel, and then to the external one.
(4) If surrounding rock is poor and unfavorable, it is necessary to consolidate the strata using techniques such as ground rockbolt, cement and mortar grouting, steel pipe grouting, jet grouting with high pressure, pile, ground freezing. Meanwhile, ground surface and water should also be treated with a proper method as well so as to keep tunneling safe.
(5) The structural design and construction technique for the ultra-shallow tunnel in an expressway in Sichuan province turns out to be a great success, and can be used to guide the design and construction of other super-shallow tunnels under similar situations.

Acknowledgments The work is financially supported by the National Natural Science Foundation of China (No. 51378436) and the Fundamental Research Funds for the Central Universities (SWJTU11ZT33).

References

1. Goodman RE, Heuze HE, Bureau GJ (1997) On modeling techniques for the study of tunnels in jointed rock. 14th symposium on rock mechanics, pp 441–479
2. Shen B, Barton N (1997) The disturbed zone around tunnels in jointed rock masses. Int J Rock Mech Min Sci 34(1):117–125
3. Zhou XJ, Li ZL, Yang CY, Gao Y (2006) Rock pressure on tunnel with shallow depth in geologically inclined bedding strata. J Southwest Jiaotong Univ (English edition) 14(1):52–62
4. Zhou XJ, Yang CY (2007) Asymmetric rock pressure on shallow tunnel in strata with inclined ground surface. J Southwest Jiaotong Univ (English edition) 15(3):203–207
5. Yang XL, Jin QY, Ma J (2012) Pressure from surrounding rock of three tunnels with large section and small spacing. J Cent South Univ (English Edition) 19:2380–2385
6. He BG, Zhang ZQ, Chen Y (2012) Unsymmetrical load effect of geologically inclined bedding strata on tunnels of passenger dedicated lines. J Mod Transp 21(1):24–30
7. Zhou XJ (2011) Study on calculation of rock pressure and determination of depth for shallow asymmetric tunnel. Adv Mater Res 261–263:1034–1038
8. Zhou XJ, Gao B, Gao Y (2005) Safety study on tunnel with shallow depth in geologically oblique bedding strata. Prog Saf Sci Technol 5:869–875
9. Zhou XJ, Gao Y, Li ZL, Yang CY (2006) Experimental study on the uneven rock pressure and its distribution applied on a tunnel embedded in geologically bedding strata. Mod Tunn Technol 43(1):12–21 (in Chinese)
10. Bhawani Singh, Goel RK (2011) Engineering rockmass classification. Butterworth-Heinemann
11. Wu AQ, Liu FZ (2012) Advancement and application of the standard of engineering classification of rock masses. Chin J Rock Mech Eng 31(8):1513–1523 (in Chinese)
12. Hack R (1997) Rock mass strength by rock mass classification. South African rock engineering congress. Johannesburg, pp 346–356
13. Jaeger JC, Cook NGW, Zimmerman RW (2007) Fundamentals of rock mechanics, 4th edn. Blackwell Publishing Ltd, Oxford
14. Sheng MR (2000) Rock mass mechanics. Tongji University Press, Shanghai (in Chinese)
15. Vocational standard of the P.R.C. Code for design of highway tunnel (JTGD70-2004). China communication press, Beijing, 2004 (in Chinese)
16. Vocational standard of the P.R.C. Code for design of railway tunnel (TB10003-2005). China railway press, Beijing 2005 (in Chinese)
17. Goel RK, Bhawani Singh, Zhao J (2011) Underground infrastructures: planning, design and construction. Butterworth-Heinemann
18. Gioda G, Locatelli L (1999) Back Analysis of the measurements performed during the excavation of a shallow tunnel in sand. Int J Numer Anal Meth Geomech 23:1407–1425
19. Chehade FH, Shahrour I (2008) Numerical analysis of the interaction between twin tunnels: influence of the relative position and construction procedure. Tunn Undergr Space Technol 23:210–214
20. Miura K, Yagi H, Shiroma H, Takekuni K (2003) Study on design and construction method for the New Tomei-Meishin expressway tunnels. Tunn Undergr Space Technol 18:271–281